Journal of Photochemistry and Photobiology A: Chemistry 222 (2011) 203–209

Contents lists available at ScienceDirect

Journal of Photochemistry and Photobiology A: Chemistry

journal homepage: www.elsevier.com/locate/jphotochem

Synthesis and characterization of novel cyclometalated iridium(III) complexes for nanocrystalline TiO_2-based dye-sensitized solar cells

Yoshiki Shinpuku, Fumiaki Inui, Misaki Nakai, Yasuo Nakabayashi*

Department of Chemistry and Materials Engineering, Faculty of Chemistry, Materials and Bioengineering, Kansai University, 3-3-35 Yamate-cho, Suita, Osaka 564-8680, Japan

ARTICLE INFO

Article history:
Received 12 February 2011
Received in revised form 23 April 2011
Accepted 10 May 2011
Available online 6 June 2011

Keywords:
Cyclometalated iridium(III) complex
Terpyridine derivative
Ligand-to-ligand charge trasfer
Dye-sensitized solar cell

ABSTRACT

Four novel cyclometalated iridium(III) complexes with the following general formulas were synthesized and characterized using ^{1}H NMR, {^{1}H–^{1}H} COSY, ESI-MS spectral and elemental analysis data: [Ir(C^N^C)(ptpy-COOH)]$^+$ (C^N^C = 2,6-diphenylpyridinato (**1**); 2,4,6-triphenylpyridinato (**2**), ptpy-COOH = 4′-(4-carboxyphenyl)-2,2′:6′,2″-terpyridine) and [Ir(C^N^C)(tpy-COOH)]$^+$ (C^N^C = 2,6-diphenylpyridinato (**3**); 2,6-ditolylpyridinato (**4**), tpy-COOH = 4′-carboxy-2,2′:6′,2″-terpyridine). The photophysical and redox properties and photovoltaic performance of the Ir(III) complexes as photosensitizers in nanocrystalline TiO_2-based solar cells were studied and compared to those of *cis*-diisothiocyanatobis(4,4′-dicarboxy-2,2′-bipyridine)ruthenium(II) (**N3**). Dye **4** exhibits the highest photovoltaic performance with an overall solar energy conversion efficiency of 2.16%.

1. Introduction

Dye-sensitized solar cells (DSSCs) have attracted considerable attention because they use inexpensive absorber materials for the conversion of sunlight into electricity [1–6]. The most efficient devices have used Ru(II) polypyridine complexes, whose lowest energy excited states are metal-to-ligand charge transfer (MLCT) states, and possess carboxyl groups for anchoring on nanocrystalline TiO_2 surface [7–12].

Compared with other transition metal complexes, cyclometalated Ir(III) complexes have attracted great attention because of the strong spin-orbit coupling of the Ir ion, high quantum yield in organic solvent, and tunable emission wavelengths from blue to red. Additionally, it has been reported that the cyclometalated Ir(III) complexes such as [Ir(C^N)$_2$(N^N)]$^+$ (C^N = cyclometalating ligand, N^N = polypyridine) have both MLCT and ligand-to-ligand charge transfer (LLCT) bands [13–17]. The combination of cyclometalating ligands with a third-row metal ion may result in enhanced mixing of the singlet and triplet excited states via spin-orbit coupling and reduced Stokes shifts between absorption and emission maxima in complexes where the lowest excited state is MLCT or LLCT in character [14,15]. Especially, for an LLCT transition, it is expected that increased spatial separation of the dye cation from the electrode surface may be possible without significantly affecting the injection efficiencies provided the electron injection occurs from an LLCT state to the TiO_2 conduction band [15]. Additionally, through variation in the nature of the cyclometalating ligand, members of this family of Ir(III) complexes may be shown to span a wide range of the visible spectrum.

The lifetimes of cyclometalated Ir(III) complexes are as long as those of compounds that are used in organic light-emitting diodes (OLEDs) [16,17]. What is more, some cyclometalated Ir(III) complexes are known to have significantly longer-lived excited states than [Ru(bpy)$_3$]$^{2+}$ [18]. This is expected to be advantageous for long-range charge-transfer reactions originating from these states, simply because the inherent excited-state decay processes are less competitive. In addition, cyclometalated Ir(III) complexes have ground-state formal redox potentials ($E^{\circ\prime}$ for Ir(III/IV) couples) that are sufficiently positive to oxidized the I_3^-/I^- redox couple. Furthermore, the excited-state formal redox potentials ($E^{\circ\prime}$ * for Ir(III/IV) couples) of the Ir dyes are quite similar to the Ru analog, indicating that these complexes should readily inject electrons into TiO_2. Therefore, cyclometalated Ir(III) complexes are expected to possess sufficient driving force for electron injection from the excited dyes to the TiO_2 conduction band. However, the reported device using the cyclometalated Ir(III) complex with 2,2′-bipyridine derivative such as [Ir(ppz)$_2$(dcbpy)]$^+$ (ppz = 1-phenylpyrazolyl, dcbpy = 4,4′-dicarboxy-2,2′-bipyridine) showed insufficient light-harvesting efficiency because [Ir(ppz)$_2$(dcbpy)]$^+$ exhibits an LLCT-based absorption at relatively high energy (455 nm) with a low molar extinction coefficient (700 M^{-1} cm^{-1}) [15]. Similarly, a dye-sensitized photoelectrode based on the cyclometalated Ir(III) complex [Ir(ppy)$_2$(dcbpy)]$^+$ (ppy = 1-phenylpyridine) with an absorption at relatively high energy (413 nm) displayed a small molar extinction coefficient (2549 M^{-1} cm^{-1}) that was as high as 2.86% (compared with 6.80% for the ruthenium dye N719) [19].

* Corresponding author. Tel.: +81 6 6368 0895; fax: +81 6 6330 3770.
E-mail address: yasuon@kansai-u.ac.jp (Y. Nakabayashi).

1010-6030/$ – see front matter © 2011 Elsevier B.V. All rights reserved.
doi:10.1016/j.jphotochem.2011.05.023

To modify the defect, the cyclometalated Ir(III) complexes with terpyridine derivatives were synthesized, indicating that these complexes have high molar extinction coefficients in the longer-wavelength region (around 520 nm, $10^4\ M^{-1}\ cm^{-1}$) [20,21] and high power-conversion efficiency. Therefore, because Ir(III) complexes with tridentate ligands are definitely superior to those with bidentate ligands, the former complexes may be applicable as sensitizers for DSSCs.

In this study, we report here on the synthesis and characterization of four novel cyclometalated Ir(III) complexes: [Ir(C^N^C)(ptpy-COOH)]$^+$ (C^N^C = 2,6-diphenylpyridinato (dpp, **1**); 2,4,6-triphenylpyridinato (tpp, **2**), ptpy-COOH = 4′-(4-carboxyphenyl)-2,2′:6′,2″-terpyridine) and [Ir(C^N^C)(tpy-COOH)]$^+$ (C^N^C = 2,6-diphenylpyridinato (dpp, **3**); 2,6-ditolylpyridinato (dtp, **4**), tpy-COOH = 4′-carboxy-2,2′:6′,2″-terpyridine). Because the cyclometalating ligands are strong electron-donors, it is interesting to investigate how these ligands affect the electronic transitions and redox potentials of complexes **1**–**4**. In addition, we evaluate the photovoltaic performance of the dye-sensitized photoelectrodes containing these Ir(III) complexes.

2. Experimental

2.1. Materials

$IrCl_3{\bullet}3H_2O$, 2,6-diphenylpyridine (dpp), 2,6-ditolylpyridine (dtp) and ferrocene were obtained from Wako Pure Chemical Industries. Tetra-n-butylammonium perchlorate (TBAP) and N-methylpyrrolidone were obtained from Tokyo Chemical Industry, and TBAP was recrystallized from acetonitorile before use. Poly(vinylidene fluoride), graphite nanopowder and cis-diisothiocyanatobis(4,4′-dicarboxy-2,2′-bipyridine)ruthenium(II) (**N3**) were obtained from Aldrich. TiO_2 paste (PECC-K01) was obtained from Peccell Technologies. All other reagents and solvents were of guaranteed grade or better and were used as received.

2.2. Synthesis of compounds

2.2.1. 4′-(4-Methoxycarboxyphenyl)-2,2′:6′,2″-terpyridine (ptpy-COOMe)

2-Acetylpyridine (2.68 g, 22.1 mmol), 4-formylbenzoic acid methyl ester (1.78 g, 10.8 mmol), and sodium hydroxide (0.900 g, 22.5 mmol) were mixed in a mortar with a pestle, and the yellow mixture was ground until it became a brown powder. The powder was transferred to a suspension of ammonium acetate (15.0 g, excess) in acetic acid (99.7%, 50 mL) and refluxed for 5 h. The crude product was precipitated from solution via the addition of water, collected by filtration and washed with water and ethanol. The precipitate was then recrystallized from $CHCl_3$/ethanol, filtered and washed with ethanol. Upon drying under vacuum, the desired product was obtained as a white solid. Yield: 38%. ^{1}H NMR (270 MHz, $CDCl_3$, 25 °C, TMS): δ (ppm) 8.76, 2H, s; 8.74, 2H, d (J = 4.6 Hz); 8.68, 2H, d (J = 8.1 Hz); 8.18, 2H, d (J = 8.1 Hz); 7.96, 2H, d (J = 10.8 Hz); 7.89, 2H, t (J = 8.7 Hz); 7.37, 2H, t (J = 5.7 Hz); 3.97, 3H, s.

2.2.2. 4′-(2-Furyl)-2,2′:6′,2″-terpyridine

This compound was synthesized according to minor modifications of previously published methods [22]. 2-Acetylpyridine (4.84 g, 40.0 mmol), 2-furaldehyde (1.93 g, 20.0 mmol), and sodium hydroxide (1.60 g, 40 mmol) were mixed in a mortar with a pestle, and the yellow mixture was ground until it became a brown powder. The powder was transferred to a suspension of ammonium acetate (15.0 g, excess) in acetic acid (99.7%, 50 mL) and refluxed for 6 h. The crude product was precipitated from solution via the addition of water, collected by filtration and washed with water and ethanol. The precipitate was then recrystallized from chloroform/ethanol, filtered and washed with ethanol. Upon drying under vacuum, the desired product was obtained as a white solid. Yield: 19%. ^{1}H NMR (270 MHz, $CDCl_3$, 25 °C, TMS): δ (ppm) 8.73, 2H, d (J = 5.6 Hz); 8.70, 2H, s; 8.63, 2H, d (J = 8.0 Hz); 7.88, 2H, t (J = 8.3 Hz); 7.60, 1H, m; 7.37, 2H, t (J = 6.1 Hz); 7.13, 1H, d (J = 3.4 Hz); 6.57, 1H, m.

2.2.3. 4′-Carboxyl-2,2′:6′,2″-terpyridine (tpy-COOH)

Potassium permanganate (4.95 g, 31.3 mmol) was added to a warm mixture of 4′-(2-furyl)-2,2′:6′,2″-terpyridine (1.06 g, 2.42 mmol), tert-butanol (145 mL), and H_2O (30 mL). The mixture was filtered through Celite after heating at reflux for 24 h, and the filtrate was reduced to ca. 50 mL. The solution was then adjusted to pH 6–7 with 2 M HCl; the product precipitated and was collected by filtration. Tpy-COOH was isolated as a white solid. Yield: 48%. ^{1}H NMR (270 MHz, DMSO-d_6, 25 °C, TMS): δ (ppm) 8.86, 2H, s; 8.76, 2H, d (J = 4.1 Hz); 8.66, 2H, d (J = 8.1 Hz); 8.04, 2H, t (J = 7.7 Hz); 7.54, 2H, t (J = 6.1 Hz).

2.2.4. 4′-(4-Methoxycarboxyl)-2,2′:6′,2″-terpyridine (tpy-COOMe)

Sulfuric acid (98%, 1 mL) was added to a suspension of tpy-COOH (0.456 g, 1.65 mmol) in absolute methanol (150 mL). After 24 h of refluxing, the reaction mixture was allowed to cool to room temperature. The solution was then adjusted to pH 6–7 with saturated aqueous $NaHCO_3$ solution and methanol was removed by evaporation. The white precipitate was filtered and washed with H_2O. Tpy-COOMe was isolated as a white solid. Yield: 97%. ^{1}H NMR (270 MHz, $CDCl_3$, 25 °C, TMS): δ (ppm) 8.99, 2H, s; 8.75, 2H, d (J = 3.9 Hz); 8.62, 2H, d (J = 7.8 Hz); 7.88, 2H, t (J = 7.6 Hz); 7.37, 2H, t (J = 5.8 Hz); 4.02, 3H, s.

2.2.5. 1-(2-Phenyl-2-oxoethyl)pyridinium iodide

Acetophenone (10.0 g, 79.4 mmol) was added to a solution of I_2 (10.1 g, 78.7 mmol) in pyridine (60 mL), and the reaction mixture was refluxed for 4 h [23]. A precipitate formed upon cooling to room temperature and was collected by vacuum filtration, washed with ether to give a light brown solid and dried in air. Yield: 63%. ^{1}H NMR (270 MHz, $CDCl_3$, 25 °C, TMS): δ (ppm) 9.00, 2H, d (J = 6.5 Hz); 8.74, 1H, dt (J = 7.8, 1.2 Hz); 8.28, 2H, t (J = 6.8 Hz); 8.07, 2H, m; 7.80, 1H, m; 7.66, 2H, m; 6.49, 2H, s.

2.2.6. 2,4,6-Triphenylpyridine (tpp)

Ammonium acetate (50.0 g, excess) was added to a stirred solution of 1-(2-phenyl-2-oxoethyl)pyridinium iodide (16.7 g, 51.4 mmol) and trans-chalcone (12.0 g, 54.1 mmol) in methanol (70 mL), and the mixture was refluxed for 4 h [23]. The precipitate that formed upon cooling was collected by vacuum filtration and washed with methanol to give a white solid, which was dried in air. Yield: 38%. ^{1}H NMR (400 MHz, $CDCl_3$, 25 °C, TMS): δ (ppm) 8.25, 4H, d (J = 8.5 Hz); 7.29, 2H, s; 7.82, 2H, m; 7.51, 9H, m.

2.2.7. [$IrCl_3$(ptpy-COOMe)]

$IrCl_3{\cdot}3H_2O$ (2.16 g, 5.54 mmol) was added to a solution of ptpy-COOMe (2.21 g, 6.02 mmol) in DMF (30 mL). The dark brown reaction mixture was heated at 120 °C for 6 h, producing a reddish brown precipitate that was collected by filtration and washed with $CHCl_3$ (3 mL × 30 mL), leading to a red powder. Yield: 92%. ^{1}H NMR (270 MHz, DMSO-d_6, 25 °C, TMS): δ (ppm) 9.21, 2H, d (J = 4.0 Hz); 9.16, 2H, s; 8.92, 2H, d (J = 8.1 Hz); 8.29, 6H, m; 7.98, 2H, t (J = 8.0 Hz); 3.92, 3H, s.

2.2.8. [$IrCl_3$(tpy-COOMe)]

This complex was prepared by a procedure identical to that used to produce [$IrCl_3$(ptpy-COOMe)] except that tpy-COOMe was used

here instead of ptpy-COOMe. Yield: 79%. ^{1}H NMR (270 MHz, DMSO-d_6, 25 °C, TMS): δ (ppm) 9.22, 2H, d (J = 5.3 Hz); 9.15, 2H, s; 8.98, 2H, d (J = 8.0 Hz); 8.28, 2H, t (J = 7.8 Hz); 8.01, 2H, t (J = 6.5 Hz); 4.07, 3H, s.

2.2.9. [Ir(dpp)(ptpy-COOH)]CF_3SO_3 (**1**)

A mixture of [$IrCl_3$(ptpy-COOMe)] (0.326 g, 0.489 mmol), dpp (0.119 g, 0.515 mmol), $AgNO_3$ (0.465 g, excess), and 1,2-ethanediol (50 mL) was refluxed for 24 h under argon in the absence of direct light. After cooling, the suspension was filtered through Celite to remove AgCl and the black byproduct. The Celite plug was washed with methanol. The organic solution was extracted with water and $CHCl_3$. The aqueous layer was discarded and the organic layer was evaporated to dryness. The crude product was purified using column chromatography on a silica gel stationary phase using an eluent mixture composed of CH_3CN/saturated aqueous CF_3SO_3Na (30:1, v/v). The first eluted orange band was evaporated to dryness. The residue was dissolved in methanol (100 mL) by the addition of aqueous 1 M NaOH (40 mL). The solution was heated at 80 °C for 6 h. After cooling to room temperature, the solution was adjusted to pH 6–7 with 2 M HCl, and water evaporated. The pure red solid (**1**) was precipitated by the addition of water and was collected by filtration. The crude product was recrystallized from $CH_3CN/C_6H_5CH_3$, collected by filtration and dried in air. Yield: 10%. Anal. Calcd for $C_{40}H_{26}N_4F_3O_5SIr$: C, 52.00; H, 2.84; N, 6.06%. Found: C, 51.52; H, 2.98; N, 5.72%. ^{1}H NMR (270 MHz, DMSO-d_6, 25 °C, TMS): δ (ppm) 9.49, 2H, s; 9.09, 2H, d (J = 7.8 Hz); 8.51, 2H, d (J = 8.4 Hz); 8.18, 7H, m; 7.94, 2H, d (J = 7.8 Hz); 7.76, 2H, d (J = 5.4 Hz); 7.41, 2H, t (J = 6.8 Hz); 6.94, 2H, t (J = 7.3 Hz); 6.71, 2H, t (J = 7.3 Hz); 6.17, 2H, d (J = 6.2 Hz). MS (ESI): m/z 775.2 ([M – CF_3SO_3]$^+$ requires 775.2).

2.2.10. [Ir(tpp)(ptpy-COOH)]CF_3SO_3 (**2**)

This complex was prepared using a procedure that is identical to that used for complex **1** except that tpp was used here instead of dpp. Yield: 30%. Anal. Calcd for $C_{46}H_{30}F_3N_4O_5SIr$: C, 55.25; H, 3.02; N, 5.60%. Found: C, 55.09; H, 2.93; N, 5.56%. ^{1}H NMR (400 MHz, DMSO-d_6, 25 °C, TMS): δ (ppm) 8.98, 2H, s; 8.65, 2H, d (J = 4.0 Hz); 8.34, 2H, d (J = 4.0 Hz); 8.30, 2H, s; 8.26, 2H, d (J = 4.1 Hz); 8.11, 2H, d (J = 4.1 Hz); 7.98 4H, m; 7.87, 2H, d (J = 3.2 Hz); 7.66, 3H, m; 7.27, 2H, t (J = 6.4 Hz); 6.99, 2H, t (J = 6.8 Hz); 6.76, 2H, t (J = 6.0 Hz); 6.27, 2H, d (J = 3.9 Hz). MS (ESI): m/z 851.0 ([M – CF_3SO_3]$^+$ requires 851.0).

2.2.11. [Ir(dpp)(tpy-COOH)]$PF_6{\cdot}C_6H_5CH_3{\cdot}CH_3CN$ (**3**)

This complex was prepared by a procedure identical to that used for complex **1** except that [$IrCl_3$(tpy-COOMe)] and KPF_6 were used here instead of [$IrCl_3$(ptpy-COOMe)] and CF_3SO_3Na. Yield: 11%. Anal. Calcd for $C_{33}H_{22}N_4O_2F_6PIr{\cdot}C_9H_{11}N$: C, 51.64; H, 3.40; N, 7.17%. Found: C, 52.19; H, 3.03; N, 6.79%. ^{1}H NMR (400 MHz, DMSO-d_6, 25 °C, TMS): δ (ppm) 9.34, 2H, s; 9.01, 2H, d (J = 7.6 Hz); 8.17, 5H, m; 8.03, 2H, t (J = 7.6 Hz); 7.93, 2H, d (J = 7.8 Hz); 7.74, 2H, d (J = 5.6 Hz); 7.38, 2H, t (J = 7.3 Hz); 6.93, 2H, t (J = 7.3 Hz); 6.68, 2H, t (J = 7.3 Hz); 6.08, 2H, d (J = 7.1 Hz). MS (ESI): m/z 699.1 ([M – PF_6]$^+$ requires 699.2).

2.2.12. [Ir(dtp)(tpy-COOH)]PF_6 (**4**)

This complex was prepared using a procedure that is identical to that used for complex **3** except that dtp was used here instead of dpp. Yield: 16%. Anal. Calcd for $C_{35}H_{26}{\cdot}N_4O_2F_6PIr$: C, 48.22; H, 3.01; N, 6.43%. Found: C, 48.92; H, 3.48; N, 6.21%. ^{1}H NMR (400 MHz, DMSO-d_6, 25 °C, TMS): δ (ppm) 9.35, 2H, s; 9.02, 2H, d (J = 7.6 Hz); 8.07, 5H, m; 7.80, 2H, d (J = 7.8 Hz); 7.72, 2H, d (J = 5.4 Hz); 7.40, 2H, t (J = 6.1 Hz); 6.73, 2H, d (J = 7.8 Hz); 5.85, 2H, s; 1.87, 6H, s. MS (ESI): m/z 727.2 ([M – PF_6]$^+$ requires 727.0).

2.3. Measurements

2.3.1. Analytical measurements

UV–visible (UV–vis) spectra were recorded on a Jasco V-670 spectrophotometer equipped with a temperature controller. Emission spectra were obtained on a Jasco 6500 spectrofluorimeter. ^{1}H NMR spectra in $CDCl_3$ or DMSO-d_6 were recorded on a JEOL JNM-EX 270 or GX 400 MHz spectrometer, and all chemical shifts were quoted with respect to TMS. Cyclic voltammetry was performed using an Als/chi electrochemical analyzer model 600A with a 20-mL one-compartment three-electrode electrochemical cell (BAS VC-3). A three-electrode system was used with a 3-mm diameter glassy carbon working electrode (BAS OD: 6 mm ID: 3 mm), an Ag/Ag^+ (Ag/0.01 M $AgNO_3$ in CH_3CN containing 0.1 M TBAP) reference electrode (BAS RE-7) and a platinum wire counter electrode. Cyclic voltammetric measurements were performed in N_2-purged CH_3CN, in which the concentrations of the complex and supporting electrolytes (TBAP) were maintained at 0.3 mM and 0.1 M, respectively. All redox potentials ($E_{1/2}$) were calculated using $(E_{pa} + E_{pc})/2$ at a scan rate of 0.1 V s^{-1} and were reported relative to a ferrocene/ferrocenium (Fc/Fc^+) couple used as an external standard. Electrospray ionization mass spectrometry (ESI-MS) was accomplished using an RSQ7000. The emission lifetimes were measured with a streak camera (C4334, HAMAMATSU) that was equipped with a monochromator (C5094, HAMAMATSU) pumped at 388 nm by a Ti:Sapphire laser system (CPA-2001, Clark-MXR) with an operating wavelength of approximately 680 nm a repetition frequency of 1 kHz was used for the femtosecond laser.

2.3.2. Preparation of the dye-sensitized TiO_2 electrodes

Nanocrystalline TiO_2 films that were approximately 20 μm thick were prepared on a conducting indium/tin oxide (ITO) glass support. Coating of the TiO_2 surface with the dye was accomplished by dipping the electrode (maintained at 60 °C) into a 0.5 mM solution of the Ir(III) complex in CH_3CN or **N3** in ethanol for 5 h. After the dye adsorption was completed, the electrode was withdrawn from the solution and dried under a stream of air. The amount of adsorbed dye was determined by desorbing the dye from the TiO_2 surface into a solution 0.5 M NaOH in ethanol/H_2O (1:1, v/v) and measuring its UV–vis absorption spectrum.

2.3.3. Photoelectrochemical measurements

The regenerative photoelectrochemical cell was fabricated by sandwiching dye-coated TiO_2 film with a thin graphite powder coated conductive glass support serves as counter electrode while iodine/iodide (0.6 M 2,3-dimethyl-1-propyl-imidazolium iodide, 0.1 M LiI, and 0.05 M I_2 in propionitrile/tetrahydrofuran (80:20, v/v)) employing as redox electrolyte. The electrodes were clipped together and illuminated through the TiO_2-sensitized surface. The counter electrode was prepared as follows. Graphite nanopowder (1.00 g) was dispersed in 2.2 mL of N-methylpyrrolidone. Poly(vinylidene fluoride) (10.0 mg) used as an adhesive was dissolved in this dispersion. The carbon paste was coated onto the conductive ITO conductivity glass substrate using a doctor blade technique and was dried at 200 °C for 1 h. An AM 1.5 solar simulator (CEP-2000, BUNKOUKEIKI) was used as the irradiation source for the photocurrent density–voltage (J–V) and the photocurrent action spectral measurements. A xenon lamp was served as a light source in conjunction with a 420 nm cutoff filter to remove ultraviolet radiation.

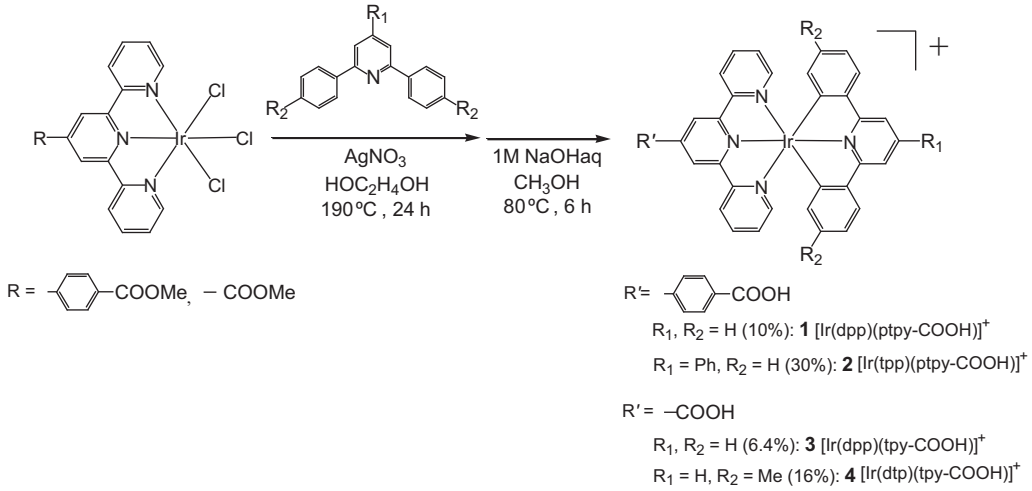

Scheme 1. Synthetic routes to Ir(III) complexes **1**–**4**.

3. Results and discussion

3.1. Synthesis and characterization of 1–4

As shown in Scheme 1, cyclometalated Ir(III) complexes [Ir(dpp)(ptpy-COOH)]$^+$ (**1**), [Ir(tpp)(ptpy-COOH)]$^+$ (**2**), [Ir(dpp)(tpy-COOH)]$^+$ (**3**), and [Ir(dtp)(tpy-COOH)]$^+$ (**4**) were synthesized as follows. First, a mixture of $IrCl_3{\cdot}3H_2O$ and ptpy-COOMe or tpy-COOMe in DMF was heated at 120 °C for 6 h. Second, a mixture of the appropriate Ir(III) precursor, diphenylpyridine derivative (dpp, dtp, or tpp) and $AgNO_3$ was refluxed in 1,2-ethanediol for 24 h. Finally, the ester groups of the cyclometalated complexes were converted to carboxyl groups by hydroxide ions. The ester link was formed between the carboxyl group of ptpy-COOH or tpy-COOMe and 1,2-ethanediol as the solvent if the conversion did not occur. The yield for the second step may be dependent on the reaction time or extending π system of the cyclometalating ligand.

Complexes **1**–**4** were characterized by UV–vis, ^{1}H NMR and $\{^1H–^1H\}$ COSY spectroscopy, and elemental analysis. $\{^1H–^1H\}$ COSY spectroscopy is a particularly convenient tool for monitoring these complexes because cyclometalation has a dramatic influence on the proton on the C_{aryl} atom bound to Ir(III) center. Representative $\{^1H–^1H\}$ COSY spectra of **1** and **2** are shown in Fig. 1. The rings and atoms of **1** and **2** labeling and the signals fully assigned by ^{1}H NMR and $\{^1H–^1H\}$ COSY spectroscopy are shown in Scheme 2. The same number and pattern of signals in the ^{1}H NMR spectra of **1**–**4** in DMSO-d_6 confirm the presence of ptpy-COOH and CN̂Ĉ ligands in a 1:1 ratio. Notably, characteristic singlets due to the ptpy-COOH unit are observed at 9.49 ppm (**1**) and 9.52 ppm (**2**); whereas, signals due to the tpy-COOH unit are observed at 9.34 ppm (**3**) and 9.35 ppm (**4**), respectively. The proton resonance corresponding to the C_{aryl} atom consists of two triplets and one doublet and is observed at approximately 7 ppm, indicating that the cyclometalation results in a significant increase in electron density on the ligand [13–20,24–26]. Notably, the proton resonance corresponding to the C_{aryl} atom peaks of **4** is observed under 6 ppm, suggesting that the methyl group, an electron-donating group is introduced in dpp unit. The phenyl group incorporated on dpp unit of **2** is observed as two triplets at 7.62 ppm (J = 7.2 Hz, 1H) and 7.72 ppm (J = 7.2 Hz, 2H), and a doublet at 8.32 ppm (J = 7.8 Hz, 1H).

Indisputable structural assignments of **1**–**4** would arise from the crystallographic analysis of single-crystals; however, it has far been impossible to obtain single-crystals suitable for X-ray crys-

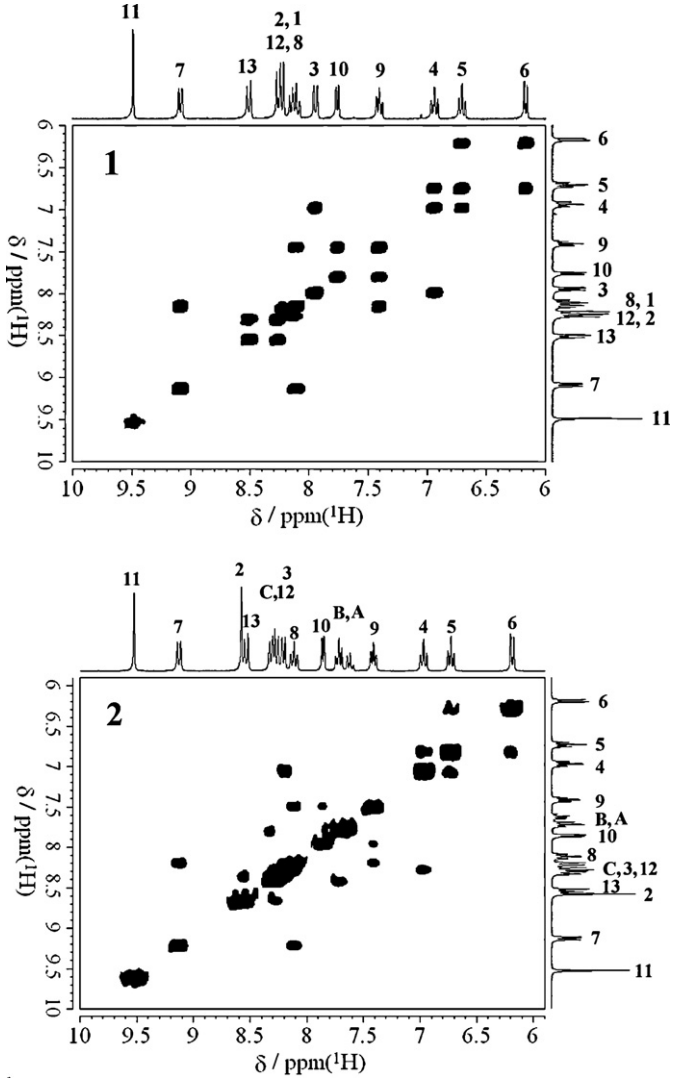

Fig. 1. Aromatic region of 270 MHz $\{^1H–^1H\}$ COSY spectra of **1** and **2** in DMSO-d_6; chemical shifts in δ ppm.

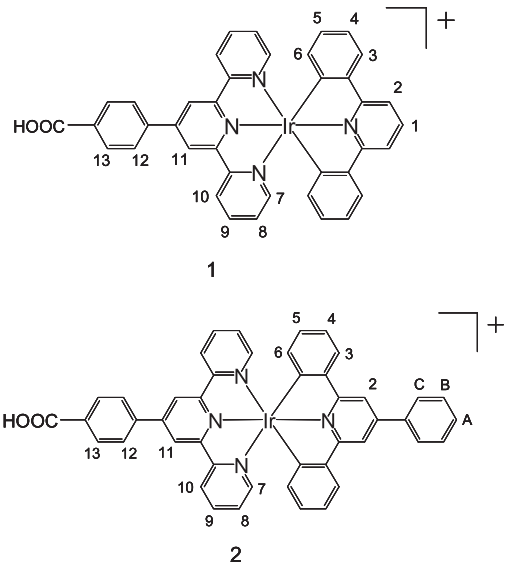

Scheme 2. Ir(III) complexes **1** and **2** with ring and atom labeling for ^{1}H NMR spectra.

tallographic analysis of any of the newly synthesized complexes. To conclude, although the structures of **1**–**4** have not been proven beyond any doubt, the structures depicted in Scheme 2 are consistent with ^{1}H NMR data described in Section 2.

3.2. Photophysical properties

UV–vis absorption and emission spectra of **1**–**4** and **N3** are shown in Fig. 2 and their data are summarized in Table 1. The bands between 400 and 550 nm are assigned to mixed MLCT ($d_{Ir} \rightarrow \pi^*_{ptpy\text{-}COOH}$) and LLCT ($\pi_{dpp} \rightarrow \pi^*_{ptpy\text{-}COOH}$; $\pi_{tpp} \rightarrow \pi^*_{ptpy\text{-}COOH}$) transitions [20,21]. The absorption and emission energies of **1**–**4** are much lower than those of cationic phenylpyrazole-based Ir(III) polypyridine complexes, used as active materials in single-layer light-emitting electrochemical cells [17] with $[Ir(ppz)_2(dcbpy)]^+$ as a sensitizer [15]. This is due to the destabilizing effect of two cyclometalated carbons on donor orbitals and the corresponding lower energy for the acceptor orbital of tpy compared to that of bpy [17]. On the contrary, the absorption and emission energies of **1**–**4** are much higher than those of **N3** because the splitting of the 5d orbital level of Ir(III) is smaller than the splitting of the 4d orbital level of Ru(II). However, the molar extinction coefficient of **1** or **2** is as large as that of **N3**. Mixed MLCT and LLCT bands of **4** lead to 10 nm red shifts compared to other Ir(III) complexes, suggesting that this is due

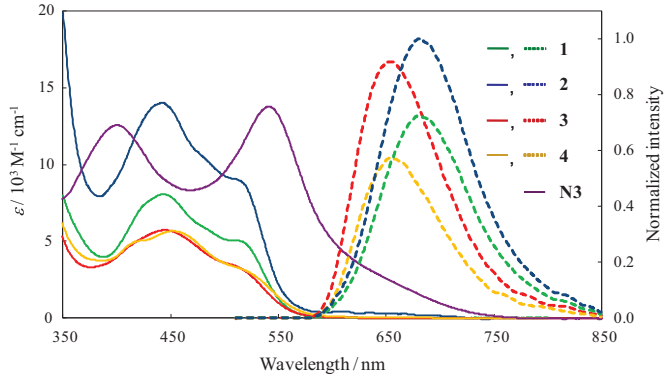

Fig. 2. UV–vis absorption (left) and emission (right) spectra of Ir(III) complexes in CH_3CN and **N3** in DMSO.

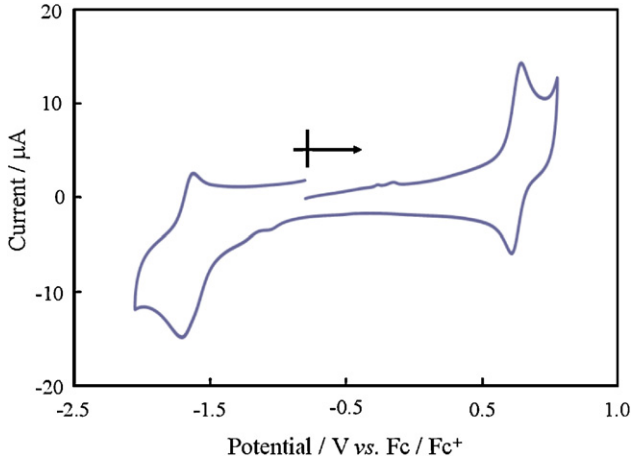

Fig. 3. Cyclic voltammogram of 0.3 mM **1** (scan rate 0.1 V s^{-1}) in deaerated CH_3CN containing 0.1 M TBAP.

to the stabilization of the HOMO that is attributed to electron-donation of the methyl group introduced in the dpp unit. The relative magnitude of molar extinction coefficients (**3** ≈ **4** < **1** < **2**) may be attributable to the contribution of the phenyl group on the ligand system leading to more delocalized MLCT and LLCT states [26]. The room-temperature emission energies (λ_{em} = 674 nm (**1**), 681 nm (**2**), 653 nm (**3**), 654 nm (**4**)) are much lower than those of the corresponding bis-tpy complexes (e.g., λ_{em} = 506 nm for the $[Ir(tolylterpyridine)_2]^+$) [27] and the bis-cyclometalated complexes (e.g., λ_{em} = 604 nm for $[Ir(ppz)_2(dcbpy)]^+$) [15]. This is due to the destabilizing effect of two cyclometalated carbons on the donor orbitals and the lower energy of the tpy acceptor orbital, as noticed previously in the discussion of the absorption spectral data. Accordingly, it is considered that the main charge displacements for **1**–**4** occur from the dpp or tpp ligand to the ptpy-COOH ligand.

The lifetimes and the emission properties of excited states for **1**–**4** in aerated CH_3CN at room temperature are also shown in Table 1. The data points were measured using a laser pulse (λ_{ex} = 388 nm) and indicate that the Ir(III) complexes have the following excited-state lifetimes: **1**; 197 ns, **2**; 216 ns, **3**; 185 ns, **4**; 183 ns at 298 K. These values are much longer than the lifetime of **N3** (50 ns at 77 K) and are as long as those of Pt(II) sensitizers [28]. Consequently, we expect that **1**–**4**, with longer lifetimes, provide the driving force for the electron injection from the excited dyes into the TiO_2 conduction band in DSSCs.

3.3. Redox properties

Complexes **1**–**4** exhibit two reversible electrochemical processes. A typical cyclic voltammogram of **1** in CH_3CN is shown in Fig. 3. Electrochemical data for **1**–**4** and **N3** are also summarized in Table 1. At negative potentials there are single one-electron processes at −1.69 V (**1**, **2**), −1.76 V (**3**), and −1.78 V (**4**) vs. Fc/Fc$^+$, which are assigned to the reductions of ptpy-COOH and tpy-COOH ligands.

The reduction potentials of **3** and **4** are thus more negative than those of **1** and **2**. The decrease in the $E_{1/2}$ values for **3** and **4** may be attributed to the carboxyl group directly introduced on terpyridine unit. These potentials are more negative than the potential of the bis(tolylterpyridine) analog, which has a reduction at 1.16 V vs. Fc/Fc$^+$ (0.35 V vs. SCE in CH_3CN). This is due to the stabilizing effect of the nearby 3+ charge on the Ir in the latter compared to the formal 1+ charge in the former [27]. Because of the destabilizing effect of two cyclometalated carbons on the donor orbitals, there are also reversible one-electron oxidation processes in the range of 0.70–0.80 V. However, each potential cannot be simply assigned to

Table 1
Spectroscopic and electrochemical data of **1**, **2**, **3**, **4**, [Ir(ppz)(dcbpy)]$^+$, and **N3** at 298 K.

Complex	λ_{abs}[a]/nm ($\varepsilon \times 10^{-3}$/M^{-1} cm^{-1})	$E_{1/2}$[b]/V vs. Fc/Fc$^+$ (ΔE_p/mV)	λ_{em}[a]/nm	τ_{em}[a]/ns	HOMO[c]/eV	LUMO[d]/eV	$\Delta G_{L\text{-}H}$/eV
1	445 (8.15) 477 (6.33) 510 (5.31)	−1.69 (62) 0.74 (79)	679	197	5.55	3.48	2.07
2	444 (14.0) 483 (10.4) 513 (9.15)	−1.69 (63) 0.70 (76)	685	216	5.50	3.47	2.07
3	448 (5.64) 482 (4.41) 512 (3.29)	−1.76 (76) 0.79 (73)	654	185	5.58	3.61	1.97
4	421 (5.04) 459 (5.60) 526 (2.85)	−1.78 (70) 0.75 (68)	653	183	5.57	3.62	1.95
[Ir(ppz)(dcbpy)]$^+$[e]	455 (0.7)	–	604	300	5.65	3.19	2.46
N3	400 (12.6) 541 (13.8)	0.44 (60)[f]	Weak	50[g]	5.24	3.54	1.70

[a] Measured in CH_3CN.
[b] Measured in CH_3CN containing 0.1 M TBAP.
[c] The energy levels of the HOMOs are estimated with the following formula: HOMO (eV) = $E_{1/2} - E_{Fc/Fc+} + 4.8$.
[d] LUMO = HOMO − $\Delta G_{LUMO-HOMO}$ (where $\Delta G_{LUMO-HOMO}$ is the absorption onset estimated from the electronic absorption spectrum of the sensitizer).
[e] Ref. [15] (dcbpy = 4,4′-dicarboxy-2,2′-bipyridine).
[f] Measured in deaerated CH_3CN/DMF (80/20, v/v).
[g] Ref. [11].

Ir oxidation, due to the strong covalency of the Ir–C bonds. It was previously shown that the HOMOs of cyclometalated Ir(III) complexes both containing dpp-type ligand and tpy-type ligands are substantially delocalized over the Ir-dpp fragment [20,21]. The oxidation potential of **1** (0.74 V) is more positive than that of **2** (0.70 V), which suggests that this difference follows the expected trend due to the introduction of the phenyl group as an electron-donor. The difference in the oxidation potentials between **3** and **4** is explained by similar reasoning as above.

3.4. Energy levels

The energy levels of the frontier orbitals of dye molecules play an important role in the electron-transfer processes in DSSCs [29]. The energy levels of HOMOs and LUMOs are derived from the oxidation potentials and the absorption onset of these dyes (Table 1). Dyes **1** and **2** have approximately the same energy gaps between HOMO and LUMO because they have close absorption onset (see Fig. 2). The energy gaps of **3** and **4** are smaller than those of **1** and **2**, suggesting that the energy levels of LUMO for **3** and **4** decrease as a result of the carboxyl group introduced on the terpyridine unit (tpy-COOH). In addition, the energy gap of **4** is smaller than that of **3** due to the introduction of methyl group into the cyclometalating ligand (Table 1). The energy levels of the HOMOs of all of the Ir(III) complexes are lower in energy than the redox potential of iodine (4.96 eV) and the energy levels of LUMOs of those are higher than TiO_2 conduction band edge (3.96 eV). It is therefore expected that all of the Ir(III) complexes possess the driving force necessary for electron injection from the excited Ir(III) dyes into TiO_2 conduction band.

3.5. Cell performance

Typical photocurrent action spectra obtained with sandwich cells using 2,3-dimethyl-1-propylimidazolium iodide (0.6 M), LiI (0.1 M) and I_2 (0.05 M) in propionitrile/tetrahydrofuran (80:20, v/v) as electrolyte solution are shown in Fig. 4.

The incident monochromatic photon-to-current conversion efficiency (IPCE) data for dye-sensitizers are plotted as a function of excitation wavelengths and exhibit a strikingly exhibit high efficiency of 63% for **4** and 70% for **N3** at 540 nm, respectively. The IPCE spectra of these dyes are consistent with the absorption spectra on the TiO_2 film. The light harvesting efficiency (LHE) can be related to the molar extinction coefficient by the following equation:

$$\mathrm{LHE}(\lambda) = 1\text{–}10^{-1000\varepsilon\Gamma} \quad (1)$$

where Γ is the surface coverage in mol cm^{-2} and ε is the molar extinction coefficient of the dye in M^{-1} cm^{-1} at wavelength λ [11,20].

The quantum yield (ϕ) for conversion of absorbed photons to current in DSSCs can be calculated via the following equation:

$$\phi(\lambda) = \frac{\mathrm{IPCE}(\lambda)}{\mathrm{LHE}(\lambda)} \quad (2)$$

The calculated LHE at 540 nm are 0.72 for **4** and 0.99 for **N3**, respectively. However, the IPCE of **4** at 540 nm is approximately the same as that of **N3**, suggesting that the recombination of injected electrons injected to TiO_2 and dye cations may be attenuated by excitation into LLCT states, which are spatially separated in nature, and that the quantum yields of Ir(III) complexes are higher than that of **N3**. Consequently, the calculated quantum yields at 540 nm were 0.98, 0.48, 0.86, 0.88, and 0.72 for complexes **1**, **2**, **3**, **4**, and **N3**, respectively. Among **1**, **2**, **3** and **4**, the quantum yield of **2** is the lowest, indicating that there are nonradiative deactivation process caused by the aggregation from the π–π stacking of the phenyl group in the cyclometalating ligand.

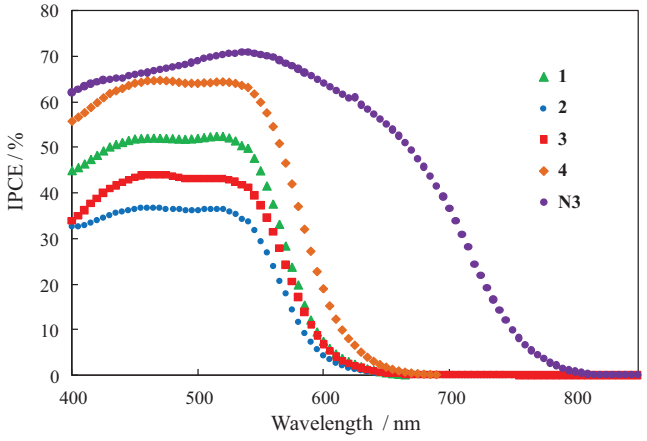

Fig. 4. Photocurrent action spectra of TiO_2 electrodes sensitized by the dyes.

Table 2
Performance parameters of dye-sensitized solar cells.

Complex	J_{sc}/mA cm^2	V_{oc}/V	*FF*	η/%	Γ^a/nmol cm^2
1	5.63	0.395	51	1.14	128
2	3.87	0.366	47	0.67	124
3	4.66	0.404	57	1.07	173
4	8.23	0.456	58	2.16	271
N3	14.1	0.463	51	3.32	146

[a] Amounts of a dye adsorbed on TiO_2 film.

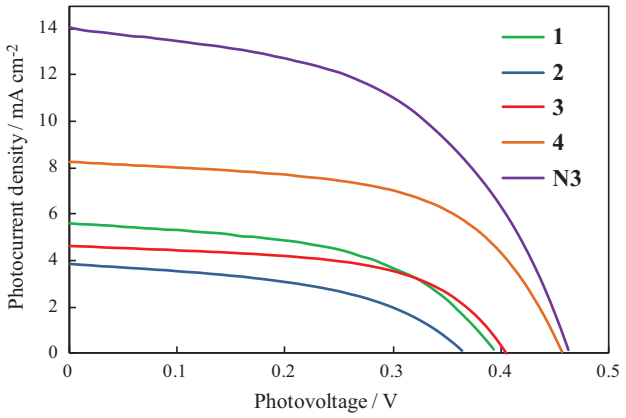

Fig. 5. Photocurrent–voltage curves for DSSCs based on Ir(III) complexes and **N3**.

The photoelectrochemical properties of dye-sensitized TiO_2 electrodes under the irradiation of AM 1.5 (100 mW cm^{-2}) irradiation are listed in Table 2, while the corresponding photocurrent–voltage curves are shown in Fig. 5. Table 2 reports the short-circuit photocurrent density (J_{sc}), open-circuit voltage (V_{oc}), fill factor (*FF*), and overall cell efficiency (η) values for representative samples investigated in this study. The electrolyte containing tetrahydrofuran improves the FF and V_{oc} of the devices [30]. Dye **4** shows the highest conversion efficiency of 2.16%. The open-circuit photovoltage of **4** is dramatically higher than the other Ir(III) complexes, which enables it to form a more compact sensitizer layer on the semiconductor surface to block charge recombination [31,32]. In addition, dye **4** also shows the highest photocurrent density in the Ir(III) complexes, relative to the amounts of adsorption. This suggests that the highest conversion efficiency of dye **4** may be attributed to amounts on the TiO_2 film (Table 2). Although the overall cell efficiency of **N3** (3.32%) is extremely low for these experimental conditions, the cell performance of new dyes may increase with better cell preparation.

4. Conclusions

The first examples of [Ir(C^N^C)(ptpy-COOH)]$^+$ and [Ir(C^N^C)(tpy-COOH)]$^+$ cyclometalated Ir(III) complexes [Ir(dpp)(ptpy-COOH)]$^+$ (**1**), [Ir(tpp)(ptpy-COOH)]$^+$ (**2**), [Ir(dpp)(tpy-COOH)]$^+$ (**3**) and [Ir(dtp)(tpy-COOH)]$^+$ (**4**) were synthesized and characterized using ^{1}H NMR, {^{1}H–^{1}H} COSY, ESI-MS spectral, and elemental analysis data. The electronic properties of the Ir(III) complexes were also investigated. The absorption spectra from 400 to 550 nm are assigned to mixed MLCT and LLCT transitions. The electrochemical properties of Ir(III) complexes show reversible one-electron reduction processes at −1.7 and −1.8 V vs. Fc/Fc$^+$ due to ptpy-COOH and tpy-COOH and reversible one-electron oxidation processes at 0.7 and 0.8 V due to the HOMOs of Ir(III) complexes. The excited-state lifetimes of Ir(III) complexes are approximately 200 ns in CH_3CN. A novel type of efficient iridium sensitizers with carboxyl pyridine ligands was synthesized, yielding a maximum of 66% IPCE and 2.16% power conversion efficiency under simulated AM 1.5 sunlight, which suggests that the energy conversion efficiency can be improved by fine tuning of the spectral overlap between the Ir(III) dye and the solar spectrum. Cyclometalated Ir(III) complexes may have two advantages. First, the high stability found in chelate ring systems of cyclometalated Ir(III) complexes [Ir(C^N^C)(N^N^N)]$^+$ can be ascribed to the stabilization of the overall solar energy conversion efficiency. Second, because the excited-state lifetime of cyclometalated Ir(III) complex is longer than that of **N3**, the higher overall solar energy conversion efficiency may be anticipated. Consequently, the cell performance of new dyes may increase due to better cell preparation.

Acknowledgments

The authors thank Prof. Ryuichi Arakawa of Kansai University for ESI-MS spectral measurements and Prof. Hiroyuki Aota of Kansai University for photoelectrochemical measurements.

References

[1] J.-J. Kim, H. Choi, C. Kim, M.-S. Kang, H.S. Kang, J. Ko, Chem. Mater. 21 (2009) 5719.
[2] E.C. Constable, A.H. Redondo, C.E. Housecroft, M. Neuburger, S. Schaffner, Dalton Trans. (2009) 6634.
[3] G. Boschloo, A. Hagfeldt, Acc. Chem. Res. 42 (2009) 1819.
[4] M. Yanagida, A. Islam, Y. Tachibana, G. Fujihashi, R. Katoh, H. Sugihara, H. Arakawa, New J. Chem. 26 (2002) 963.
[5] S. Ferrere, Chem. Mater. 12 (2000) 1083.
[6] G. Hasselmann, G.Z. Meyer, Phys. Chem. 212 (1999) 39.
[7] B.-S. Chen, K. Chen, Y.-H. Hong, W.-H. Liu, T.-H. Li, C.-H. Lai, P.-T. Chou, Y. Chi, G.-H. Lee, Chem. Commun. (2009) 5844.
[8] H. Choi, C. Baik, S. Kim, M.-S. Kang, X. Xu, H.S. Kang, S.O. Kang, J. Ko, M.K. Nazeeruddin, M. Grätzel, New J. Chem. 32 (2008) 2233.
[9] M. Grätzel, J. Photochem. Photobiol. C: Photochem. Rev. 4 (2003) 145.
[10] M.K. Nazeeruddin, P. Pechy, T. Renouard, S.M. Zakeeruddin, R. Humpbry-Baker, P. Comte, P. Liska, L. Cevey, E. Costa, V. Shklover, L. Spiccia, G.B. Deacon, C.A. Bignozzi, M. Grätzel, J. Am. Chem. Soc. 123 (2001) 1613.
[11] M.K. Nazeeruddin, A. Kay, L. Rodicio, R. Humpbry-Baker, E. Müller, P. Liska, N. Vlachopoulos, M. Grätzel, J. Am. Chem. Soc. 115 (1993) 6382.
[12] B. O' Regan, M. Grätzel, Nature 353 (1991) 737.
[13] K.K.-W. Lo, K.Y. Zhang, C. Chung, K.Y. Kwok, Chem. Eur. J. 13 (2007) 7110.
[14] Q. Zhao, S. Liu, M. Shi, C. Wang, M. Yu, L. Li, F. Li, T. Yi, C. Huang, Inorg. Chem. 45 (2006) 6152.
[15] E.I. Mayo, K. Kilsa, T. Tirrell, P.I. Djurovich, A. Tamayo, M.E. Thompson, N.S. Levis, H.B. Gray, Photochem. Photobiol. Sci. 5 (2006) 871.
[16] A.J. Wilkinson, H. Puschmann, J.A.K. Howard, C.E. Foster, J.A.G. Williams, Inorg. Chem. 45 (2006) 8685.
[17] A.B. Tamayo, S. Garon, T. Sajoto, P.I. Djurovich, I.M. Tsyba, R. Bau, M.E. Thompson, Inorg. Chem. 44 (2005) 8723.
[18] M.S. Lowry, J.I. Goldsmith, J.D. Slinker, R. Rohl, R.A. Pascal, G.G. Malliaras, S. Bernhard, Chem. Mater. 17 (2005) 5712.
[19] Z. Ning, Q. Zhang, W. Wua, H. Tian, J. Organomet. Chem. 694 (2009) 2705.
[20] M. Polson, M. Ravaglia, S. Fracasso, M. Garavelli, F. Scandola, Inorg. Chem. 44 (2005) 1282.
[21] M. Polson, S. Fracasso, V. Bertolasi, M. Ravaglia, F. Scandola, Inorg. Chem. 43 (2004) 1950.
[22] J. Husson, M. Beley, G. Kirsch, Tetrahedron Lett. 44 (2003) 1767.
[23] W. Zecher, F. Kröhnke, Chem. Ber. 94 (1961) 690.
[24] B.G. Paolo, R.C.D. Kiyoshi, S.A. Pavel, B.P. Curtis, Inorg. Chem. 48 (2009) 9631.
[25] K.D. Bryan, R.C.D. Kiyoshi, B.P. Curtis, Inorg. Chem. 48 (2009) 9644.
[26] S. Ott, M. Borgström, L. Hammarström, O. Johansson, Dalton Trans. (2006) 1434.
[27] P.J. Collin, M.I. Dixon, P.J. Sauvage, G.J.A. Williams, F. Barigelletti, L. Flamini, J. Am. Chem. Soc. 121 (1999) 5009.
[28] A. Islam, H. Sugihara, K. Hara, L.P. Singh, R. Katoh, M. Yanagida, Y. Takahashi, S. Murata, H. Arakawa, G. Fujihashi, Inorg. Chem. 40 (2001) 5371.
[29] M. Grätzel, J. Photochem. Photobiol. A: Chem. 3 (2004) 164.
[30] A. Fukui, R. Komiya, R. Yamanaka, A. Islam, L. Han, Solar Energy Mater. Solar Cells 90 (2006) 649.
[31] Z.-S. Wang, N. Koumura, Y. Cui, M. Takahashi, H. Sekiguchi, A. Mori, T. Kubo, A. Furube, K. Hara, Chem. Mater. 20 (2008) 3993.
[32] M. Yanagida, T. Yamaguchi, M. Kurashige, K. Hara, R. Katoh, H. Sugihara, H. Arakawa, Inorg. Chem. 42 (2003) 7921.